Marine Geophysical Researches (2005) 26:183–195
DOI 10.1007/s11001-005-3717-6

Development of a system for 3D high-resolution seismic reflection profiling on lakes

M. Scheidhauer[1,2], F. Marillier[1,*] and D. Dupuy[1]
[1]*Institute of Geophysics, University of Lausanne, Amphipole Bldg, CH-1015, Lausanne, Switzerland*
[2]*Risk Management Solutions Limited, Peninsular House, 30 Monument Street, London, EC3 8NB, UK*
**Corresponding author (Tel.: +41-0-21-692-44-02; Fax: +41-0-21-692-44-05; E-mail: Francois.Marillier@unil.ch)*

Received 12 January 2004; accepted 17 November 2005

Key words: 3D, air gun, high-resolution, Lake Geneva, Molasse, multi-channel, navigation, reflection seismics, seismic acquisition, Switzerland

Abstract

A high-resolution three-dimensional (3D) seismic reflection system for small-scale targets in lacustrine settings has been developed. Its main characteristics include navigation and shot-triggering software that fires the seismic source at regular distance intervals (max. error of 0.25 m) with real-time control on navigation using differential GPS (Global Positioning System). Receiver positions are accurately calculated (error < 0.20 m) with the aid of GPS antennas attached to the end of each of three 24-channel streamers. Two telescopic booms hold the streamers at a distance of 7.5 m from each other. With a receiver spacing of 2.5 m, the bin dimension is 1.25 m in inline and 3.75 m in crossline direction. To test the system, we conducted a 3D survey of about 1 km^2 in Lake Geneva, Switzerland, over a complex fault zone. A 5-m shot spacing resulted in a nominal fold of 6. A double-chamber bubble-cancelling 15/15 in^3 air gun (40–650 Hz) operated at 80 bars and 1 m depth gave a signal penetration of 300 m below water bottom and a best vertical resolution of 1.1 m. Processing followed a conventional scheme, but had to be adapted to the high sampling rates, and our unconventional navigation data needed conversion to industry standards. The high-quality data enabled us to construct maps of seismic horizons and fault surfaces in three dimensions. The system proves to be well adapted to investigate complex structures by providing non-aliased images of reflectors with dips up to 30°.

Introduction

High-resolution (HR) marine seismics, in exploration industry terms, typically involves frequencies up to about 1000 Hz and reaches a vertical resolution of less than a meter. This technique is widely used both in the field of engineering geophysics as well as in geological and environmental site investigations. While two-dimensional (2D) surveys became common practice, three dimensional (3D) acquisitions, which involve complex field and processing procedures, are still mainly carried out by the hydrocarbon exploration industry using much lower frequencies. From the geophysical point of view (acquisition and processing) and also from that of a geologist (interpretation), any target is in reality 3D and should be treated as such. Numerous examples from hydrocarbon exploration prove that 3D seismic reflection surveys, especially in geologically complex areas, are more appropriate than 2D surveys for accurately imaging small-scale geological changes (see Yilmaz, 2001). A "true" 3D survey adequately samples the target both in inline and crossline directions and allows migration in 3Ds of the whole data cube without spatial aliasing.

In recent years, several 3D high-frequency seismic systems were developed. Henriet et al. (1992) and Missiaen et al. (2002) designed a system for very shallow environments such as rivers providing limited penetration of less than 50 m below the water bottom. Marsset et al. (2002) proposed a marine 3D very HR acquisition system for sites of limited extent (2 km×1 km), such as dams, artificial island sites, pipeline routes on the continental shelf in water depths up to 100 m and target vertical resolutions of 1 m. Because of the limited streamer length of these systems, it is

impossible to perform a velocity analysis directly on these data. An additional longer streamer 2D survey is necessary to obtain the required detailed velocity model, especially important for complex targets. Müller et al. (2002) carried out a high-frequency survey in the Baltic Sea in order to study a fluvial channel system and shallow gas accumulations beneath unconsolidated sediments in the southern Kiel Bay. In this example, because of limited manoeuvrability of the vessel at sea conditions, the crossline spacing was often too large and led to aliasing problems.

Acquisition configurations of the above examples were chosen with respect to specific environments. The system described in this paper combines some of their advantages such as the use of several streamers to save acquisition time and the reduced-size equipment that fits on small boats and avoids their draw-backs, in order to build a 3D multi-channel and multi-streamer system adapted to small-scale 3D targets in lake environments such as river deltas, complex fault zones, etc. Because Lake Geneva has no tidal action, no strong currents and no swell noise and may have water depths of several hundred meters (late arrival of multiple energy), it forms an ideal site to evaluate the capabilities of such a system. Our equipment was designed to avoid spatial aliasing of the target horizons and to have a direct control on stacking and migration velocities. Spatial aliasing occurs when the bin size (Δx_{bin}) is:

$$\Delta X_{\mathrm{bin}} > \frac{V_{\mathrm{avg}}}{4 f_{\max} \sin \alpha_{\max}},$$

where V_{avg}: average seismic velocity to the target reflector, $f_{\max}$: highest unaliased seismic frequency in the wavelet and $\alpha_{\max}$: maximum dip in in-line direction to be imaged without aliasing.

Consequently, as the dominant frequency of the seismic source is reduced, the minimum size of the bin can be increased – and thus the distance between streamers of the acquisition system – without spatially aliasing steeply dipping structures. Furthermore, a signal of lower dominant frequency is less easily attenuated, although high frequencies are needed for good resolution. By using an air gun with a frequency bandwidth centred on 330 Hz, i.e. lower than the frequencies in the above mentioned systems, some of their very high vertical resolution of less than a meter is traded off for a deeper penetration (several hundred meters versus < 50 m below the water bottom).

We designed and built the necessary equipment or had it built according to our specifications. A 3D survey was then carried out on a test area for which acquisition parameters were optimized. This test area is located in Lake Geneva, Switzerland, near the city of Lausanne, over the offshore extension of a complex thrust fault zone.

Components of the 3D acquisition system

Figure 1 shows the general configuration of the 3D acquisition system. It consists of an air gun seismic source powered by compressed air. A program controlled by differential GPS triggers both the gun and the seismograph, and it provides real-time navigation to the ship's pilot. Seismic signals from three streamers towed behind the ship are sent to the seismograph and stored on tape. During data acquisition, air gun shots are triggered with distance at short time intervals (generally around 4–5 s), and it is therefore essential that each system component correctly operates on a continuous basis without human intervention. The combined time delay of dGPS, trigger software and firing box is estimated to be less than 100 ms implying a systematic positioning error of less that 0.1 m for the location of the reflection point. The mechanical delay of the air gun and the delay of the seismograph were measured separately and corrected accordingly.

Seismic source

We used a pneumatic bubble-cancelling Mini G.I (Sodera S.A.) air gun (Figure 2) that contains two independent chambers, the "generator" and the "injector". The first chamber generates the primary pulse. After a time delay the second chamber injects air inside the bubble that was produced by the generator in order to prevent the violent collapse of the bubble and its further oscillation. The time delay between the two pulses is empirically set in order to eliminate or strongly attenuate the seismogenic bubble oscillations.

The volume of the gun can be adapted. Frequencies of the air gun in 15/15 in^3 configuration range from approximately 40–650 Hz with a dominant frequency at 330 Hz when operated at 80 bars (M. Gros, pers. comm. 2000). The gun's far-field signature recorded without and with the

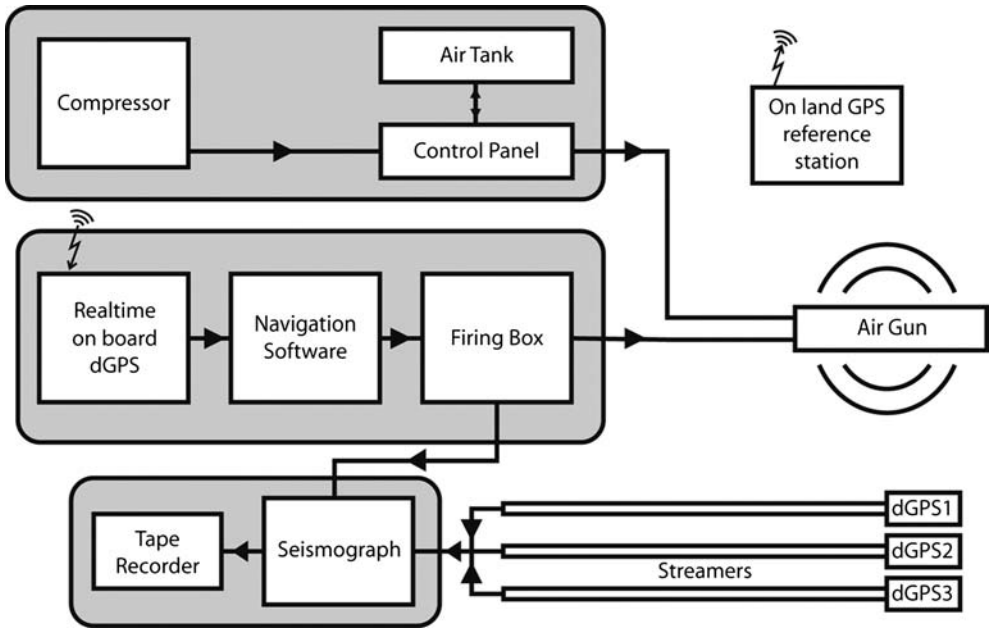

Figure 1. Schematic configuration of the 3D high-resolution seismic acquisition system.

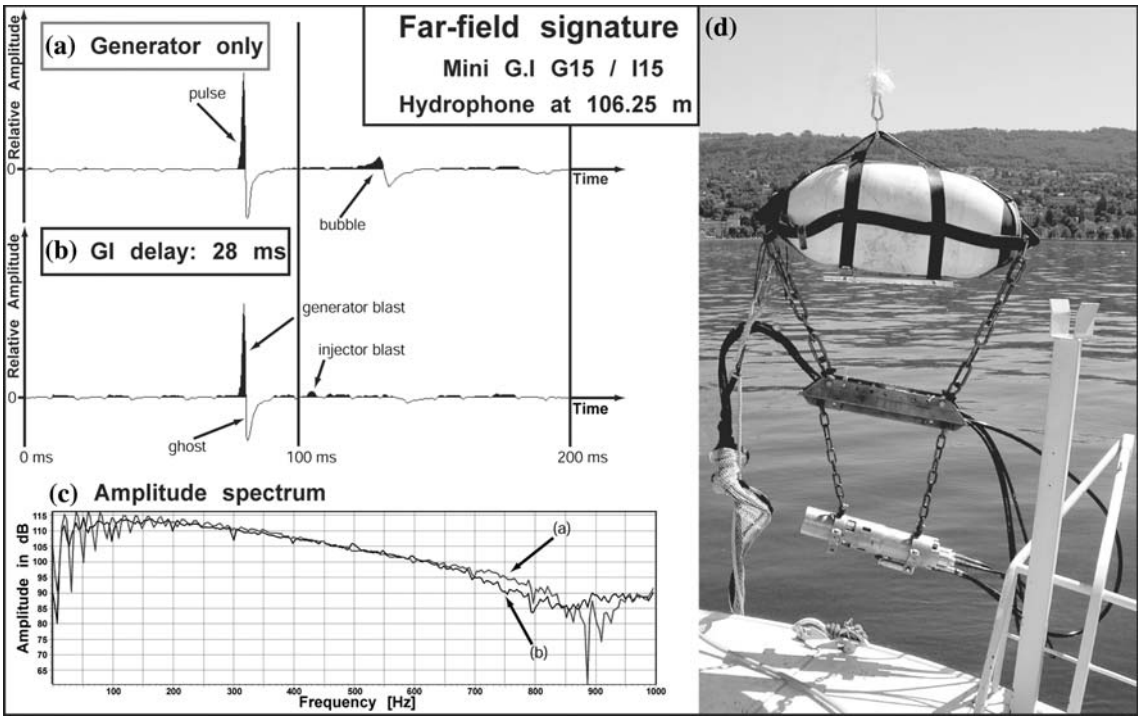

Figure 2. Unfiltered far field signature of the Mini G.I air gun (15 in^3 generator/15 in^3 injector configuration) at 106 m depth produced with the generator only (a) and with additional generator contribution at the optimum delay of 28 ms (b). Amplitude spectrum of both signatures (c). In working configuration, the Mini GI gun is attached to a buoy through an intermediate railing (d). Distance between the buoy's floatation line and the airgun is 1 m.

injector demonstrate how well the bubble oscillation (visible in Figure 2a) is nullified (Figure 2b) when the firing delay between the two chambers is set to 28 ms. For the first non-zero notch to occur beyond 650 Hz in the frequency spectrum, the gun depth should not exceed 1.15 m. To be on the safe side, the gun was put at 1 m below the surface ($f_{notch} = 750$ Hz). The spectrum of the well developed far-field signature is relatively flat between 70 and 350 Hz. The importance of low frequencies in the Mini G.I air gun's spectrum compared with other sources usually used in shallow studies such as boomers or sparkers, leads to higher signal strength and deeper penetration, at the cost of poorer vertical resolution. Moreover, the wavelet's energy is concentrated at its onset (minimum phase) and no precursor pulse such as generated by water guns, hinders determination of accurate reflection times.

Compressed air system

The high-pressure air (up to 280 bars) is generated onboard with a three-cylinder compressor (Cirrus SA, Figure 1) and a nominal capacity of 16 m^3/h. However, the actual production rate depends on the purge time-interval set to evacuate condensed water from the interior, which slows down the process. According to our experience, the average air production rate is 15 m^3/h when purging every 15–20 min. The high-pressure air is stored in a 200 l tank. A control panel directs the air supply from the compressor or from the tank to the gun. An adaptable pressure valve allows controlling the pressure in the gun.

Streamers and their towing system

Three solid state streamers were used, each containing 24 hydrophones spaced at 2.5 m with a total length of 60 m. A lead-in and a 2.5 m tail section complete each streamer and a deck cable connects them to the seismograph. A tail buoy was attached to the tail section in order to provide some tension in the streamer that straightens it. Hydrophones are equipped with preamplifiers powered by two 12 V batteries. The recordable hydrophone bandwidth ranges from 3 or 6 Hz to about 4 kHz.

An important constraint in 3D-data acquisition is the spacing between inlines that has to be chosen according to spatial sampling requirements. This, in turn, depends on the maximum structural dip of the target. Using the Mini G.I gun in the 15/15 in^3 configuration (with a maximum frequency of 650 Hz), the fixed 2.5 m spacing between the hydrophones allows unaliased imaging of dips up to 27° along the inlines. However, in the crossline direction the same spacing is generally not necessary if the main strike of the target is known beforehand and the acquisition (inline) direction can be chosen perpendicular to it.

In our system, the centre streamer is towed directly behind the gun, and the other two at a variable distance, but symmetrically from it. To keep the side streamers at their position, we designed telescopic booms and rafts to which the streamer lead-ins are attached (Figure 3). The boom itself consists of two hollow aluminium shells, one of which can slide out of the other, its extremity reaching a distance of 5–7.5 m away from the centre of the boat (Figure 3). The fixture to the boat is a combination of a car tow-hook and a trailer clutch. This allows free rotation of the boom in all directions, and it has the advantage of being easy to install and adaptable to different boats. The booms are light, easy to manoeuvre and to transport. In order to guarantee a stable position of the lead-in just below the water surface and to prevent the boom from sinking into the water, its outer end is fastened to a specially developed raft of sufficient buoyancy (see Figure 3b and c).

Navigation and positioning equipment

To obtain real-time positioning of the boat we used one onboard differential GPS (Figure 1). A reference station was set up less than 5 km away from the survey area. Signals from GPS satellites were continuously recorded during the entire length of the survey in order to post-process data from three additional GPS receivers attached to the streamers. The radio-transmitted signals from the reference station were used by the onboard (dual frequency) RTK-GPS that provides coordinates with accuracy better than ± 0.05 m. With a specially developed navigation program, the boat position was displayed in real-time on a laptop allowing accurate sailing, immediate quality control of line straightness and heading correction by the pilot (Figure 4). Boat positions and shot times are continuously recorded during seismic acquisition. The program is also designed to trigger the source at equal distance intervals. A 5 V trigger

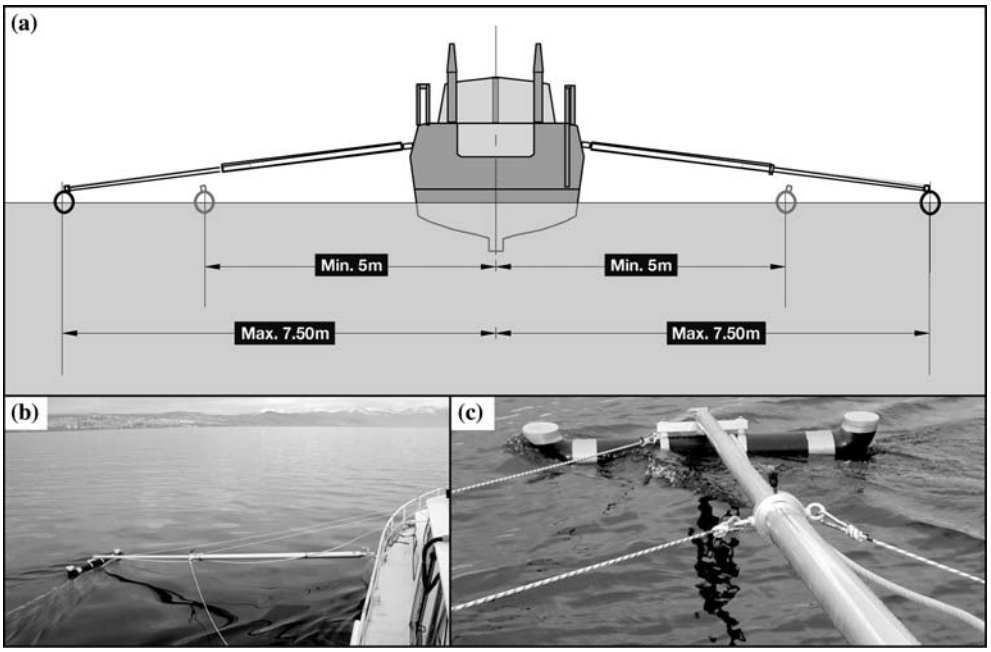

Figure 3. The streamer towing system. Schematic section of the boat with the two booms being deployed (a). Streamer lead-ins are attached to a raft that supports the end of the boom. The distance between the raft and the ship's midpoint can be adjusted from 5 to 7.5 m. Ropes allow holding the booms at a right angle to the ship (b and c). In sailing mode, the telescopic booms are collapsed and secured to the side of the boat.

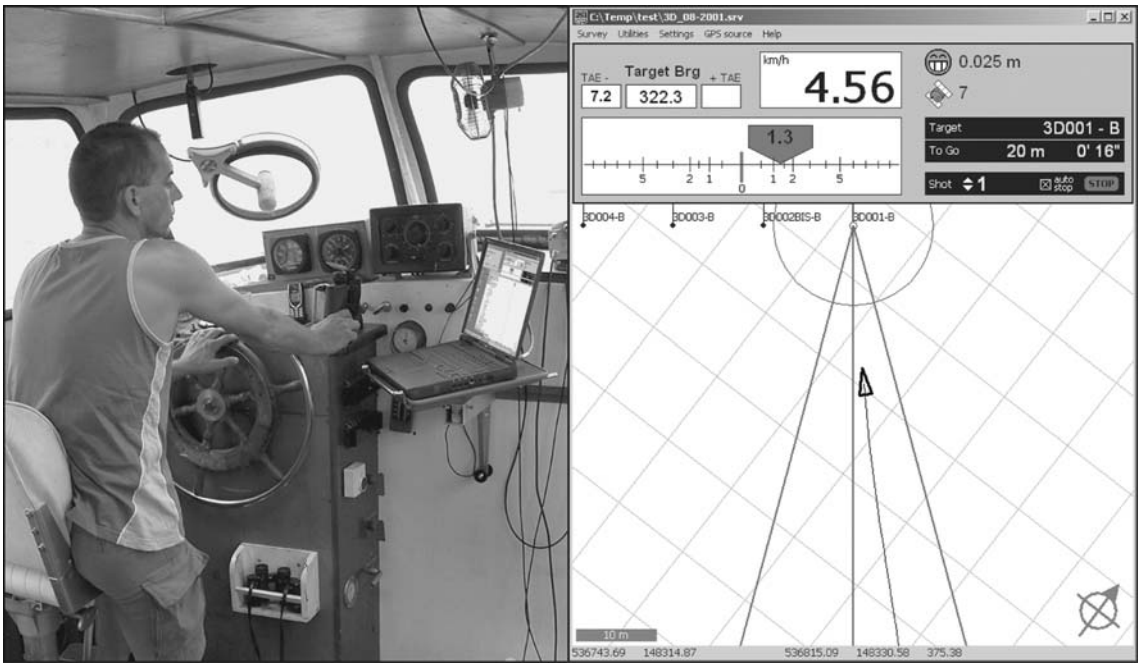

Figure 4. Setup of laptop with navigation software and screen display of the specially developed program (GPS_shot). This example shows navigation monitoring while the ship sails to the profile starting point. Top of window shows a number of navigation parameters including current target bearing, ship speed, lateral deviation from target line (large arrow), number of GPS satellites used and accuracy with which coordinates are determined.

signal is sent from the laptop to the firing box (Figure 1) where it is converted to a 90 V pulse fed to the gun. Simultaneously, a signal is sent to the seismograph to start data recording. Due to the 5 Hz dGPS coordinate reading rate and the boat's speed (about1 m/s) the maximum possible error of triggering behind the exact shot position is 0.25 m.

The size of the bin in our 3D acquisition is 1.25 m in the inline and 3.75 m in the crossline direction (see section after next). Accordingly, for reflection points to fall within the correct bin, positioning accuracy of both hydrophones and source must be less than half the bin's shortest dimension (0.625 m). Accurate determination of hydrophone positions, however, is a challenge that we partially solved with the aid of mono-frequency dGPS receivers attached to the end of each streamer. For this purpose, we constructed three rafts onto which a waterproof case was fixed that housed the GPS unit (Figure 5). The data of each instrument are stored in the receiver's memory and downloaded each evening. Processing was later carried out using frequency and phase information in cinematic mode. Smoothing of the data was possible thanks to a data density of 1 data point per second. This yields an accuracy of at least 0.2 m.

To test the accuracy of the source positioning, we carried out some additional measurements that included a dGPS on the source buoy. In good weather conditions, the standard deviation of the source position relative to an ideal source point was 0.07 m and 0.33 m in inline and crossline directions, respectively.

The seismic data were recorded with a BISON seismograph (Jupiter software) allowing a resolution of up to 24 bits. The data were continuously stored on a DAT tape drive in SEGY format.

The 3D test site

In Lake Geneva, offshore the city of Lausanne, recent high-resolution 2D investigations revealed a complex fault zone (Morend et al., 2002). This major thrust fault system, which trends southwest–northeast, is known from onshore investigations and from an oil exploration borehole north-east of Lausanne that reveal a total vertical throw of $\sim$1 km. It separates two Tertiary Molasse units, the Plateau Molasse and the Subalpine Molasse. In this area, molassic units are made of coarse and fine-grained sandstones, silty marls, and scarce clays.

The southeast-dipping Molasse beds are unconformably overlain by a relatively thin layer of subhorizontal Quaternary sediments of glacial and lacustrine origin. The fault zone represents the extension of the Paudèze Fault mapped onshore by Weidmann (1988). Although the area allows excellent penetration of seismic signals, Morend (2000) noted the difficulty of correlating complex geological structures across seismic lines only 50 m apart. This and the close vicinity to the city of Lausanne made the site well suited to test our 3D acquisition system.

We first carried out some preliminary investigations. A 2D seismic line was shot perpendicular to the strike of the fault zone (see portion of this line in Figure 10a) and it was later followed by a first 3D survey using a single 48-channel streamer and one onboard GPS receiver (Scheidhauer et al., 2000; Scheidhauer et al., 2001a, b; Beres et al., 2003). The survey covered an area of approximately 1 km^2,

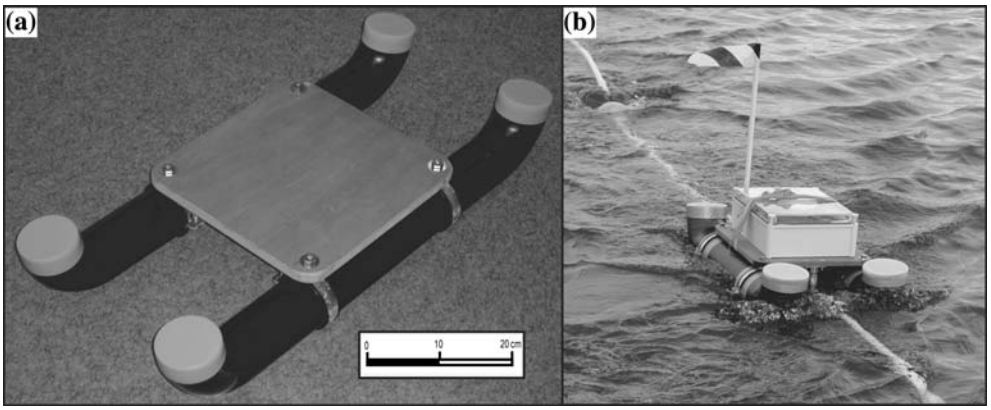

Figure 5. Raft (a) onto which dGPS receivers are attached near the end of each streamer (b).

with its longest dimension perpendicular to the strike of the fault zone. Although it provided a first 3D image of the area and was rich in experiences for the acquisition and processing of such data, the survey suffered from several shortcomings. Among those, the high frequency range of the water gun (up to 1700 Hz), produced spatially aliased dipping reflectors and the limited power of the gun prevented sufficient depth penetration (Scheidhauer, 2003).

The 3D data acquisition

Knowing the exact position of the fault zone limits and the approximate strike of the dipping Molasse strata (parallel to this limit), we outlined an area for the 3D survey centred on the fault zone and defined the acquisition direction perpendicular to it. We selected a CMP spacing of 3.75 m in crossline direction (i.e. between inlines), because this prevents spatial aliasing of dips below 9° in this direction. Our previous investigations indicated that dips up to 9° occur along strike but larger ones were not expected.

Figure 6 shows the lay-out and the dimensions of the three-streamer configuration used for the 3D data acquisition described in this paper. The retractable booms keep the two outer streamers at a distance of 7.5 m from the centre streamer to obtain the required 3.75 m crossline bin dimension. The 24-channel streamer, at 2.5 m trace spacing, results in bins of 1.25 m in the inline direction. The first hydrophone of the centre streamer is located 5 m away from the seismic source leading to a far offset of 62.5 m. A 5-m shot spacing provided a nominal fold of 6. The average boat speed of 1 m/s implied a shot interval of about 4 s. A maximum penetration depth of the order of 300 m below the lake bottom was achieved. Best vertical resolution is 1.1 m. With velocities encountered in this area, theoretical horizontal resolution is 43 m (diameter of Fresnel zone). However, this reduces to 4.5 m after migration using the dominant frequency of 330 Hz. The data of the 72 channels were recorded at 0.5 ms intervals during 1000 ms. Because the lake floor was imaged at a two-way travel time of almost 400 ms in the deepest parts of the survey, reflections down to 800 ms were unaffected by the water-bottom multiple.

We acquired 60 sail- or 180 CMP-lines in 9 days with a distance between sailed lines of 11.25 m (3×3.75 m), covering an area of about 1500 m by 650 m in the inline and crossline directions, respectively. Sailing direction was chosen to be up dip for all lines. Shooting all lines in the same direction (parallel shooting) avoids static effects that arise when dipping structures are present (Vermeer, 2002). In any case, the limited capacities of compressor and air tank prevent from continuous anti-parallel shooting. Sailing from the end of one survey line to the starting point of the next at the opposite side of the survey area provides additional time for recharging the air tank.

Data processing

The data were processed with the Géovecteur software of CGG (Compagnie Générale de Géophysique). Because this commercial processing

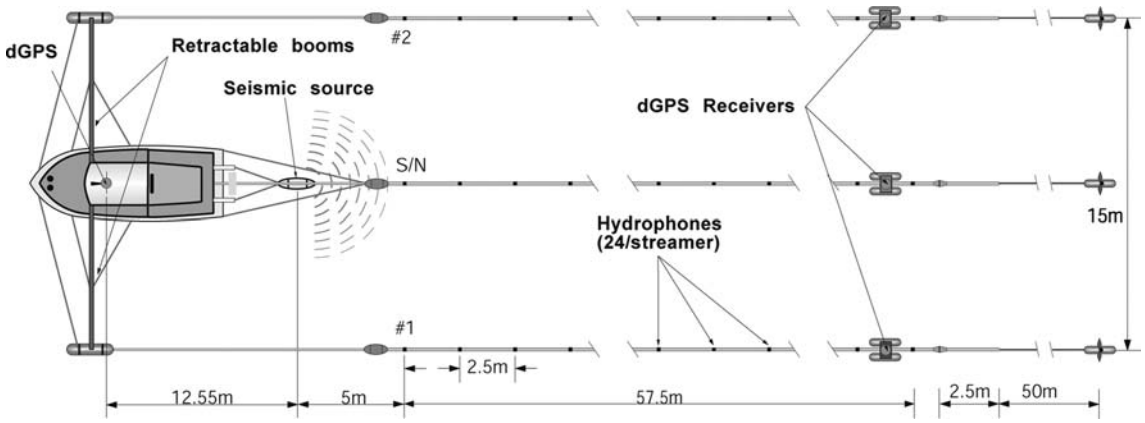

Figure 6. Multi-streamer configuration for the acquisition of seismic VHR 3D data.

software has been developed for hydrocarbon exploration industry standards, algorithms are coded according to that standard's scale and are not always adapted to high-resolution imaging. We first processed the navigation data. Computer programs had to be written to undertake necessary coordinate interpolations and to output navigation data in the right format. Positions were checked for continuity and, in places, missing data had to be simulated.

Processing then followed a conventional scheme using data organized in bins. After data formatting and seismograph and gun time-delay corrections, processed navigation data were merged with the seismic traces and geometry was assigned. Further prestack processing included trace editing, bin harmonization, spherical divergence correction, bandpass filtering and a detailed velocity analysis on DMO corrected gathers before final DMO and NMO correction and stack. The raw data volume of 11 GB was reduced to 1.8 GB after stack Post-stack processing comprised a one-pass 3D time migration in the frequency-space domain.

Bin harmonization represented an important part of the 3D processing sequence, because inaccurate boat steering and streamer feathering caused uneven coverage. In order to obtain only one trace per offset class and bin, bins were harmonized either by duplicating those traces within the same offset class that come from either one of two adjacent crossline bins or by deleting redundant traces. This method was successful in the way that only very few bins remained empty and the overall fold became close to nominal (Figure 7). Bin harmonization also significantly improved the performance of later DMO correction, a process in which reflection energy of dipping reflectors is moved to adjacent bins.

Another important processing step is the velocity analysis. The previous 3D test survey was carried out with a 48-hydrophone streamer and a maximum offset of 122.5 m. We used this data set to build a velocity model. A detailed two-step (conventional and DMO corrected) analysis was performed on a total of 600 semblance spectra computed on every second inline and every 50th CMP. Velocity picking on subsets of these semblance spectra showed that the complexity of the chosen survey site required detailed velocity information at intervals no larger than 15 m in fault strike and about 60 m in fault dip direction. Interval velocities range from 1420 m/s at the water bottom to 3000 m/s at about 410 ms. Below this time, no more velocity picking was possible due to the limited signal penetration and a lack of semblance values.

In a complex geological setting such as the Paudèze Fault Zone, accurate 3D migration is essential. Although our post-stack time migration provides acceptable results, obvious shortcomings were observed especially where strongly dipping reflectors are present (see Figure 10b). A pre-stack migration software being developed at the Ecole des Mines de Paris for oil-industry targets (Thierry et al., 1999) and adapted to near surface seismic data (Scheidhauer et al., 2003a) provided significant improvements of problematic areas in the data cube (Scheidhauer et al., 2003b). We believe that further developments in this direction will continue to enhance the quality of 3D high-resolution data.

The 3D data cube

Figure 8 presents a perspective view of the 3D data cube, while Figure 9 shows an example time slice and a vertical section. The following large-scale geological units can be recognized: the continuous beds of the Plateau Molasse in the northwest, the Paudèze Fault that separates Plateau from Subalpine Molasse and the fault zone of fractured Subalpine Molasse to the southeast. The fault zone is bounded to the southeast by "Fault B". Another fault is identified within the Plateau Molasse (Fault C). The erosional surface of the Molasse is covered by glacio-lacustrine (Pleistocene) and post-glacial lacustrine (Holocene) sediments. The maximum depth of signal penetration in this data set is illustrated by reflections within the Plateau Molasse visible even beyond 470 ms which corresponds to a penetration below water bottom of up to 300 m.

A detailed geological interpretation is out of place here and was published elsewhere (Scheidhauer et al., 2005). However, it is interesting to note that complex structures were successfully imaged, and that the 3D aspect of the fault zone is clearly illustrated. With the aid of interpretation software several horizons and fault surfaces were traced through the complete data cube. Even the delineation of a few boundaries only, gave new insight into small-scale geomorphological features and geological processes (Scheidhauer, 2003).

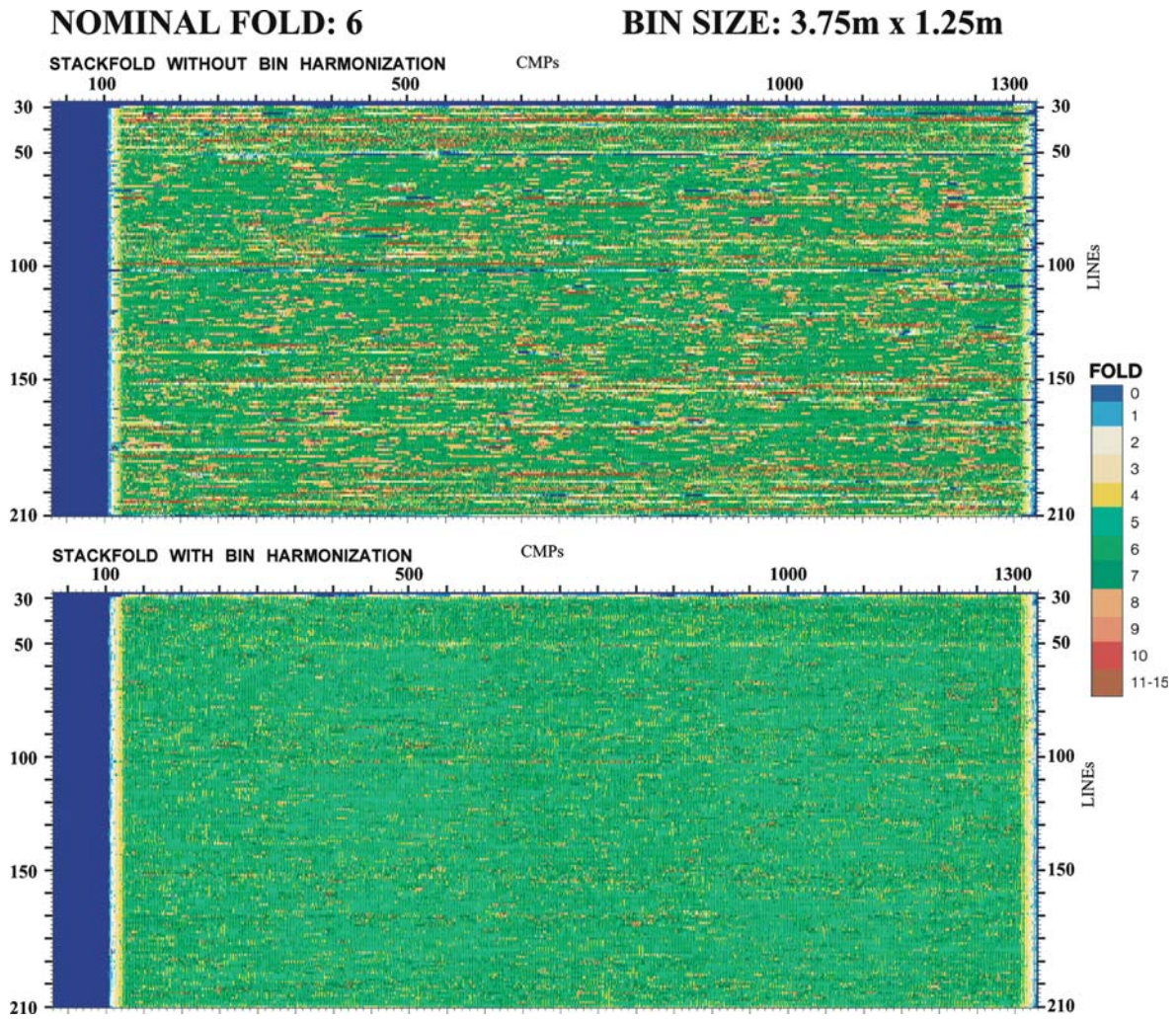

Figure 7. Stacking fold for each bin without (top) and with (bottom) application of flex binning (for explanation see text). Colour palette was adapted to associate the nominal fold of 6 with the green colour.

Examples of mapped features include the concave shape of the Paudèze Fault surface, minor thrust faults within the Plateau Molasse and a change in the direction of its bedding dip as well as a regional change in morphology of the eroded top Molasse surface (Figure 9). Three dimensional imaging of such structures revealed changes in dip direction within the same horizon and relationships between deformation of the Molasse and the fault geometry. Time slices allowed easy determination of true dips. The time slice in Figure 9a suggests that Molasse deformation postdates faulting of the Paudèze Fault Zone. In addition, reflectors in the 3D cube can be accurately followed along strike. This was not possible with the 50 m spacing of the 2D lines of Morend (2000). Although only larger-scale morphological aspects of the 3D data cube have been interpreted so far, smaller-scale features, such as on-lapping reflectors and differential erosion could be observed.

To illustrate the advances made in 3D imagery we compare a 2D section and a section extracted from the 3D data cube located at the same position (Figure 10). The first one is 12-fold and was migrated in two dimensions while the second one is 6-fold and was migrated in three dimensions. The section extracted from the 3D data cube is generally of better quality with a better signal-to-noise ratio and better reflector continuity despite its lower fold. This is, for example,

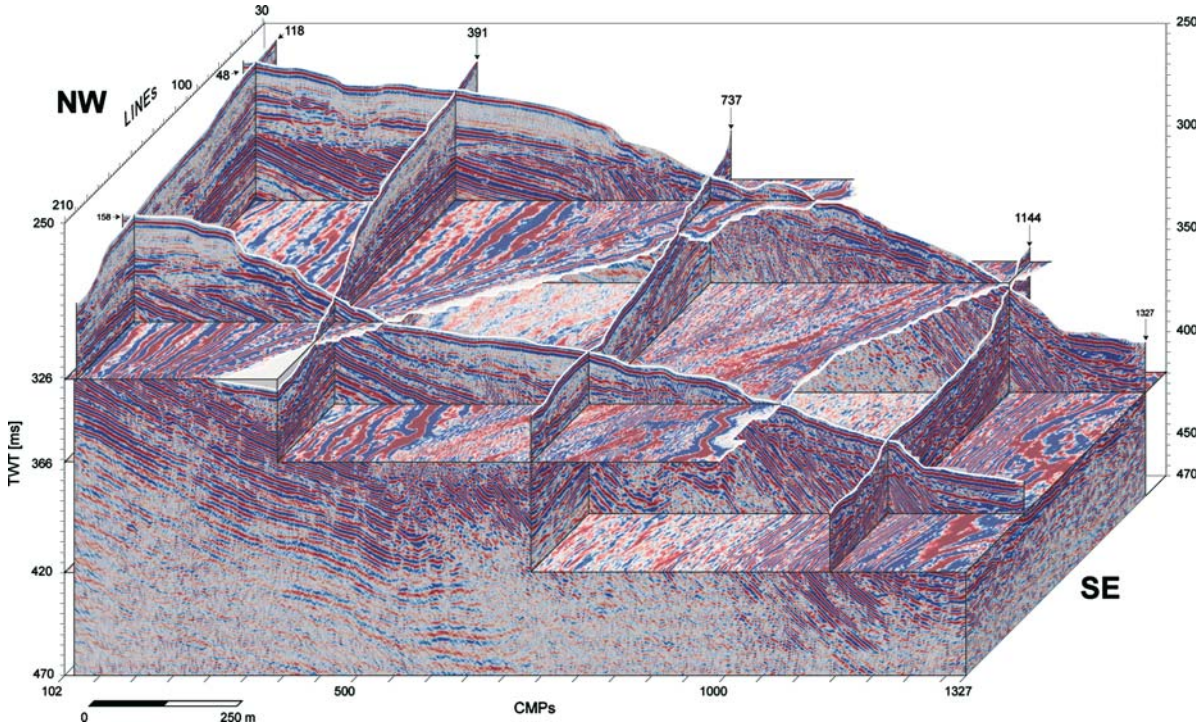

Figure 8. 3D time migrated data cube with several inlines, crosslines and times slices exposed. The continuous reflection outlining the top of the data cube corresponds to water bottom. Vertical exaggeration is approximately two.

illustrated in the Molasse unit between CMP 625 and 800 and below the Paudèze Fault that dips about 35° to the southeast. Another fault (grey arrows in Figure 10b) can be observed that was not visible in the 2D sections. Within the imaged fault zone itself (CMP 625–1000) reflectors appear (see white arrows in Figure 10b) that were barely seen in the 2D line. Details of the lake bottom are

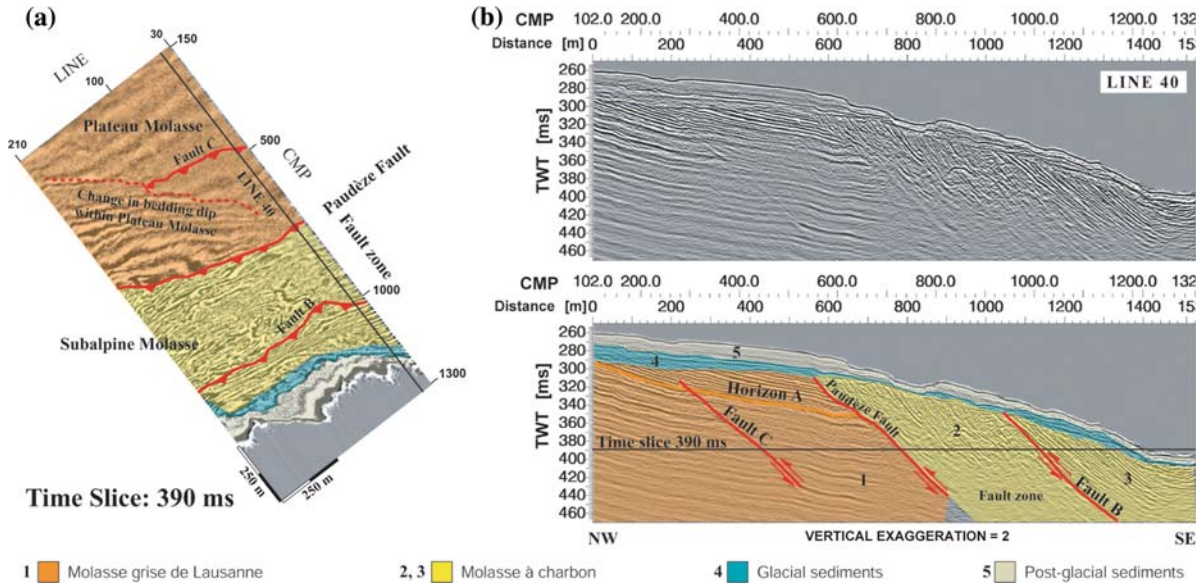

Figure 9. Time slice at 390 ms of the survey cube (a), and example of inline 40 without (top) and with interpretation (b). There is a vertical exaggeration of about two in the inline sections. The position of the time slice is indicated on inline 40 and vice versa.

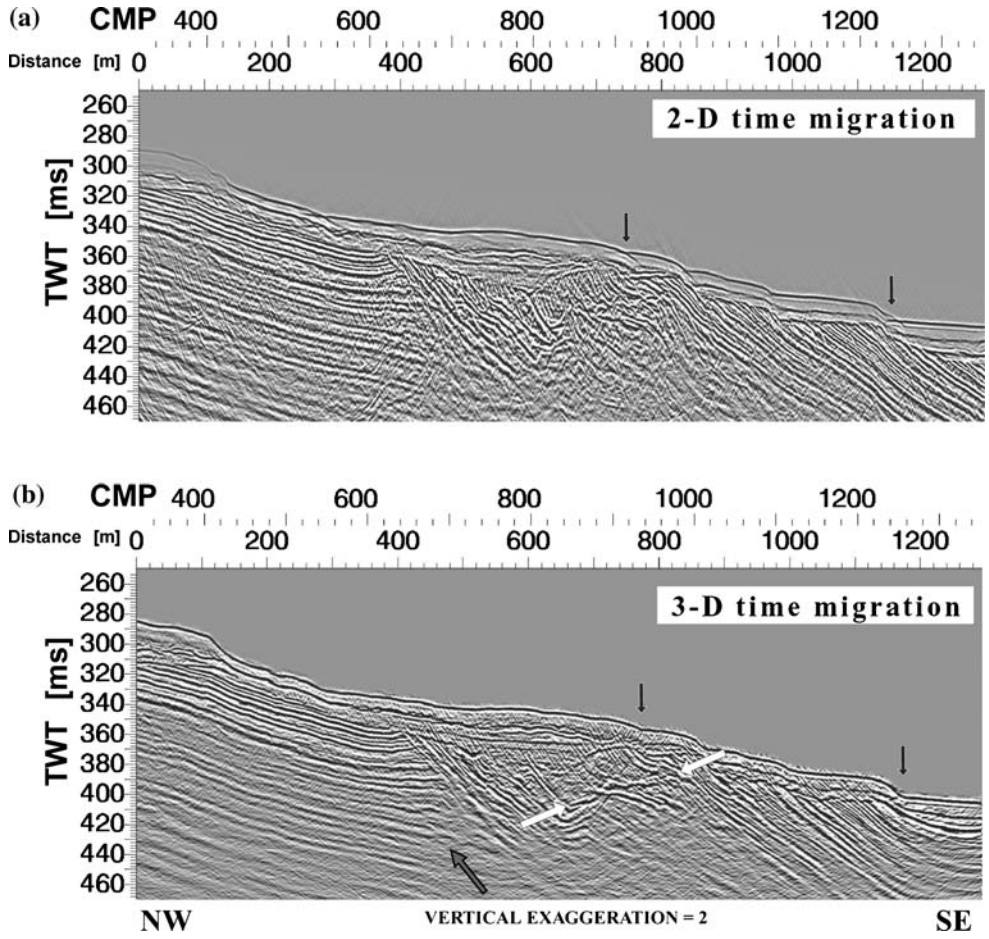

Figure 10. Comparison between two sections obtained at the same location, as part of (a) 2D and (b) 3D surveys. The section extracted from the 3D cube generally exhibits a much better quality, e.g. in areas indicated by arrows. In a few locations, artefacts are caused by the 3D time migration algorithm (see text for explanations).

much clearer in the 3D section in areas where the lake bottom reflector undulates (black arrows in Figure 10). Some negative effects of the 3D migration are, however, observed such as the small dipping artefacts in the uppermost part of the sedimentary unit (Quaternary lacustrine sediments) and the bending of the reflections below 420 ms two-way time at the extreme southeast end of the section is due to edge effects and low fold and would also appear in 2D, if the section had not originally been longer.

Conclusions

We developed an efficient high-resolution 3D multichannel seismic reflection system adapted to small-scale 3D targets in lake environments. High quality data are obtained which show particularly clean, interpretable images of complex subsurface structure in all directions.

The system makes use of a three-streamer system with two telescopic booms that hold the streamers at a distance from each other that can be varied according to the desired bin width. A dGPS-based navigation software was developed that triggers shots with distance and enables real-time control on navigation. This high-precision boat positioning is complemented by three independent dGPS units attached to each streamer tail providing positioning of the hydrophones. The Mini G.I. air gun with frequencies up to 650 Hz proved to be an appropriate source with respect to sampling requirements and signal strength, and it allowed unaliased imaging of dipping reflectors down to a depth of approximately 300 m.

Processing of high-resolution data sampled in time intervals below 1 ms and requiring a spatial precision of less than a meter turned out to be complicated because the available exploration industry software was often not adapted to this small scale. Nevertheless, a 3D conventional processing flow has been tailored to work around the software's sampling requirements and was complemented by computer programs that format the unconventional navigation data to industry standards.

Delineation of several horizons and fault surfaces in the time-migrated data reveal the potential of the new system to interpret small-scale seismostratigraphic and tectonic features in three dimensions. Preliminary tests with a 3D preserved-amplitude prestack depth-migration algorithm demonstrate that the excellent quality of this data set allows application of such sophisticated techniques even to shallow seismic surveys.

Further developments of our 3D acquisition system are envisioned. To better position the hydrophones we plan to use up to three GPSs' per streamer. Tests have demonstrated that active streamers up to three times longer (170 m) than the ones used in this study are needed to achieve better velocity analysis. Finally, in order to take advantage of seismic amplitudes, e.g. for amplitude versus offset (AVO) studies, accurate calibration of the hydrophones will be necessary.

Acknowledgements

We thank the F.A. Forel Institute, University of Geneva, for providing the ship (La Licorne) and I. Christinet and P. Arpagaus for being the pilots. P. Logean developed the navigation and gun-firing software and a program to process our unconventional navigation data. R. Wolfgang designed and built the GPS rafts and the telescopic booms. M. Beres helped develop the 3D system when it was still in its infancy and A. Rosselet was instrumental with electronic equipment testing and maintenance. Thanks are due to P.-Y. Gilliéron for lending us GPS receivers and to Y. Levet for post-processing the raw GPS data. M. Gros from SODERA helped solve many problems with the seismic sources. We are grateful to M. Weidmann for sharing with us his geological knowledge on regional geology and to D. Morend and G. Gorin for pointing out the excellent seismic response in the area that became our test site. P. Thierry ran for us his preserved-amplitude prestack depth-migration code on our 3D data cube. Special thanks to B. Marsset who introduced us to the acquisition of VHR 3D data and welcomed us on board during one of his scientific cruises. W. Versteeg helped with the initial acquisition phases of the project. Thanks are due to the numerous people who helped on the boat. F. Perret drafted some of the figures. This work was funded by the Swiss National Science Foundation with grants 21-49710.96/1 and 20-54505.98/1. The "Fondation Herbette" of the University of Lausanne helped purchase the SUN workstation on which data processing was carried out.

References

Beres, M., Scheidhauer, M. and Marillier, F., 2003, Imaging perialpine structures in Lake Geneva, Switzerland, with 3-D High-resolution seismic reflection methods. Eclogae Geologicae Helvetiae, Supplement 1 (Lake Systems - From Ice Age to Industrial Time): 31–38.

Henriet, J.P., Verschuren, M. and Versteeg, W., 1992, Very high resolution 3D seismic reflection imaging of small-scale structural deformation, *First Break* **10**(3), 81–88.

Marsset, T., Marsset, B., Thomas, Y. and Didailler, S., 2002, Sismique très haute résolution 3D: une nouvelle méthode d'imagerie des sols superficiels, *C. R. Geoscience* **334**(6), 403–408.

Missiaen, T., Versteeg, W. and Henriet, J.P., 2002, A new 3D seismic acquisition system for very high and ultra high resolution shallow water studies, *First Break* **20**(4), 227–232.

Morend, D., 2000, High-resolution seismic facies of alluvial depositional systems in the Lower Freshwater Molasse (Oligocene - early Miocene, western Swiss Molasse Basin). PhD thesis, University of Geneva, Geneva.

Morend, D., Pugin, A. and Gorin, G.E., 2002, High-resolution seismic imaging of outcropscale channels and an incised-valley system within the fluvial-dominated Lower Freshwater Molasse (Aquitanian, western Swiss Molasse Basin), *Sediment. Geol.* **149**, 245–264.

Müller, C., Milkereit, B., Bohlen, T. and Theilen, F., 2002, Towards high-resolution 3D marine seismic surveying using boomer sources, *Geophys. Prospect.* **50**(5), 517–526.

Scheidhauer, M., 2003, Development of a 3-D very high-resolution seismic reflection system for lacustrine settings – a case study over a thrust fault zone in Lake Geneva. PhD thesis, University of Lausanne, Lausanne.

Scheidhauer, M., Beres, M. and Marillier, F., 2000, Initial results of a high-resolution 3-D seismic reflection survey in north-central Lake Geneva, Switzerland. 70th Annual International Meeting: Society of Exploration Geophysicists, Expanded Abstracts, Aug. 6–11, NSG P1.7, pp. 1389–1392, Calgary, Canada.

Scheidhauer, M., Beres, M., Dupuy, D. and Marillier, F., 2001a, Studying thrust faults in Lake Geneva, Switzerland,

with high-resolution 2D/3D reflection seismics. Proceedings of 7th Meeting of Environmental & Engineering Geophysical Society, European Section, Sept. 2–6, pp. 250–251, Birmingham, England.

Scheidhauer, M., Beres, M., Dupuy, D. and Marillier, F., 2001b, A high-resolution 2D/3D seismic study of a thrust fault zone in Lake Geneva, Switzerland. European Association of Geoscientists & Engineers, 63rd Conference, Expended Abstracts, June 11–14, pp. 130, Amsterdam, The Netherlands.

Scheidhauer, M., Marillier, F. and Thierry, P., 2005, Detailed 3D seismic imaging of a fault zone beneath Lake Geneva, Switzerland. *Basin Res*. **17**, 155–169.

Scheidhauer, M., Thierry, P. and Marillier, F., 2003a, 3D prestack depth migration of very high resolution data. 65th Meeting: European Association of Geoscientists & Engineers, Extended Abstracts, June 2–5, pp. 15, Stavanger, Norway.

Scheidhauer, M., Thierry, P. and Marillier, F., 2003b, 3D very high resolution data: from acquisition to 3D prestack depth imaging. 73rd Annual International Meeting: Society of Exploration Geophysicists, Expanded Abstracts, Oct. 26–31, Dallas, USA.

Thierry, P., Lambaré, G., Podvin, P. and Noble, M.S., 1999, 3-D preserved amplitude prestack depth migration on a workstation, *Geophysics* **64**, 222–229.

Vermeer, G.J.O., 2002, 3-D Seismic Survey Design. In: Beasley, C.J. (ed.), *Geophysical References 12*. Society of Exploration Geophysicists, Tulsa, USA.

Weidmann, M., 1988, Feuille 1243 Lausanne. Atlas Géol. Suisse 1:25 000, Carte et notice expl. 85.

Yilmaz, Ö., 2001, Seismic data analysis – processing, inversion, and interpretation of seismic data, in Cooper, M.R. (Ed), Investigations in Geophysics II, 2nd ed., Society of Exploration Geophysicists, Tulsa, USA, pp. 2025.